

A rational approach for fire-resistance evaluation of double-tee, prestressed concrete slabs in parking structures

Puneet Kumar and Venkatesh K. R. Kodur

- This paper proposes a rational approach to evaluate the fire resistance of double-tee slabs in parking structures using a finite element analysis (FEA) model to analyze realistic vehicle fire scenarios and loading conditions.
- Appropriate vehicle fire scenarios were developed based on a thorough literature review, and the FEA model was validated by comparing results from the model to a fire test on a full-scale double-tee slab.
- Case studies analyzed with the proposed rational approach indicate that fire-resistance predictions for double-tee slabs under current prescriptive approaches for evaluating fire resistance are overly conservative.

Double-tee, prestressed concrete slabs offer numerous advantages over traditional slab systems in terms of higher load-carrying capacity, better use of space, cost-effectiveness, and optimized production. Consequently, the use of these slabs as a structural solution has gained popularity in recent decades. Double-tee slabs are often used in parking structures, where their longer spans reduce the total number of required columns, allowing better use of space.

The two main functions of double-tee slabs in parking structures include transferring applied surface loads to framing members and providing fire compartmentation. In the event of a fire, double-tee slabs are required to contain fire spread from one floor to another while sustaining applied loading, without collapse, for a certain fire-exposure duration; this is defined as the fire resistance of a double-tee slab. Currently, fire-resistance requirements for a double-tee slab are assessed using a prescriptive approach based only on standard fire exposure conditions, as defined by ASTM E119.¹ However, fire exposure in a parking structure often results from burning vehicles and can be significantly different from standard fire exposure. Vehicle fires are typically characterized by a rapid temperature rise and quick decay over a short duration, whereas standard fire exposure encompasses a longer burning duration and no decay phase. **Figure 1** compares the evolution of fire temperatures for two typical vehicle fires in parking structures (parking fire 1 and 2) with standard fire exposure (ASTM E119¹ fire). Figure 1 shows that temperatures in parking structure fires quickly attain higher peak temperatures and subside in a shorter amount

PCI Journal (ISSN 0887-9672) V. 65, No. 2, March–April 2020.

PCI Journal is published bimonthly by the Precast/Prestressed Concrete Institute, 200 W. Adams St., Suite 2100, Chicago, IL 60606.

Copyright © 2020, Precast/Prestressed Concrete Institute. The Precast/Prestressed Concrete Institute is not responsible for statements made by authors of papers in *PCI Journal*. Original manuscripts and discussion on published papers are accepted on review in accordance with the Precast/Prestressed Concrete Institute's peer-review process. No payment is offered.

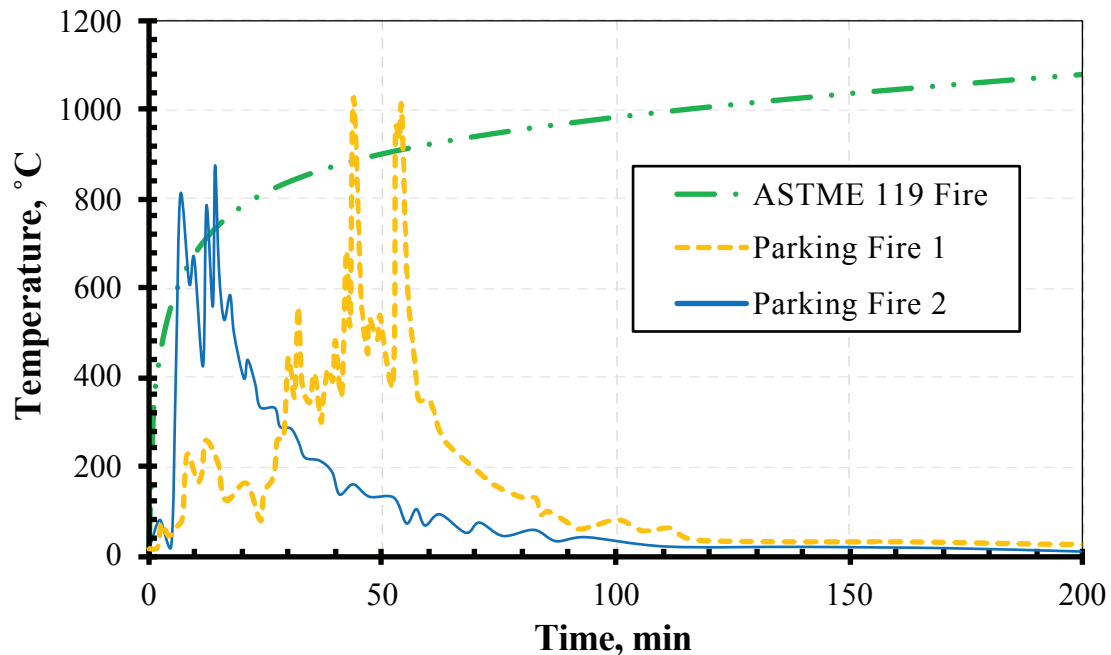


Figure 1. Evolution of fire temperatures in vehicle and standard fire exposures. Note: $^{\circ}\text{C} = (^{\circ}\text{F} - 32)/1.8$.

of time than the standard fire, thus producing less thermal impact on structural members. Therefore, the fire resistance of double-tee slabs, based on standard fire exposure, may not be a realistic indication of fire performance.

Most of the previous fire-resistance studies on double-tee slabs are based on standard fire exposure, and there is limited guidance for evaluating their fire resistance under vehicle fire exposure. The earlier studies on finite-element-based models for prestressed concrete double-tee slabs were by Franssen and Bruls.² However, this model did not account for shear stresses, and therefore, shear capacity of the slab was determined using simplified equations from prescriptive codes. Kodur and Hatinger³ developed a two-dimensional numerical model that could simulate the fire response of double-tee slabs under standard and realistic fire exposure. A series of parametric studies was carried out to characterize parameters governing the fire resistance of double-tee slabs, and it was concluded that fire scenario and failure criteria have a significant influence on the fire resistance of double-tee slabs. However, there is still a lack of validated advanced three-dimensional numerical models for tracing the thermo-mechanical behavior of double tees under realistic fire exposure from the start of the fire to burnout conditions. On the other hand, several advanced numerical models do exist in literature for other structural members, such as beams, columns, slabs, and walls.⁴⁻⁸ This lack of advanced numerical models is hindering the development of design guidelines for the fire-resistance evaluation of double-tee slabs under vehicle fire exposure.

Currently, the fire resistance of double-tee slabs is evaluated mainly through tabulated fire ratings, which are derived from standard fire tests and are a function of equivalent slab thickness and clear cover thickness to prestressing strands.^{9,10} The minimum concrete cover keeps the temperature in the prestressing strands below a critical temperature to satisfy the load-carrying functionality of the slab. The minimum slab thickness limits the temperature rise on the unexposed slab surface to satisfy compartment functionality. However, these two provisions for evaluating fire resistance are overly conservative because they do not account for all critical factors governing the fire response of double-tee slabs. As an alternative to tabulated fire ratings, design specifications also provide simplified fire design equations to evaluate the fire resistance of slabs.^{9,10} This procedure evaluates moment capacity degradation based on sectional temperatures under standard fire exposure to check for failure of the member at any given time. However, no guidance is provided on evaluating sectional temperatures under realistic vehicle fire scenarios (such as those in parking structures), which limits the applicability of the design equations to standard fire exposure.

To overcome these limitations, a rational approach was developed for evaluating the fire resistance of double-tee slabs under realistic fire and loading conditions that can occur in a parking structure. This approach considers critical factors for evaluating the fire resistance of double-tee slabs, including varying fire characteristics, member geometry, loading and support conditions, temperature-dependent material properties,

geometric and material nonlinearity, and realistic failure limit states. This rational approach was developed using a three-dimensional finite element analysis (FEA) model in structural analysis software, where the response of the slab is traced from the initial burning stage through the decay stage of the fire (burnout conditions). The applicability of this approach to double-tee slabs in parking structures is illustrated through case studies that incorporate slab dimensions, loading conditions, and fire scenarios that are typical in parking structures.

Characteristics of vehicle fires

Vehicles are made of highly combustible materials and contain significant amounts of flammable fuel at any point in time and, therefore, are prone to fire incidents due to accidental (such as electrical and mechanical malfunctions, collisions, and the like) or intentional (vandalism) causes. From 2006 to 2010, fire departments in the United States alone responded to an average of 152,300 vehicle fires per year, which caused an average of 209 civilian casualties and direct property loss of \$536 million per year.¹¹ About 69% of these fires were caused by electrical and mechanical malfunctions in vehicles, which indicates a high probability of accidental vehicle fires in parking structures. Hence, it is imperative to design parking structures to withstand the effects of such probable vehicle fires. One of the key input parameters affecting fire design is determining an appropriate fire scenario that can occur in a parking structure. Identifying a fire scenario includes defining the number of vehicles involved in the fire, the resulting fire temperatures, and the location of the fire relative to structural members.

Number of vehicles

The number of vehicles involved in a fire has a direct impact on the magnitude and evolution of fire temperatures. The spacing of the vehicles, combustible fuel in the vehicles, spread of the fuel, and ventilation conditions are the primary basis for determining the number of vehicles involved in a fire.¹² Statistics compiled on vehicle fire incidents in parking structures indicate that most involve burning of only one to three vehicles at a given time, and most fires last for less than one hour.¹²⁻¹⁴ Joyeux et al.¹³ compiled vehicle fire statistics in Europe from 1995 to 1997 and reported that 96% of vehicle fires in underground parking structures involved only one to three vehicles and about 95% of them lasted less than one hour. In addition, all fires in open parking structures involved fewer than three vehicles and all lasted for less than one hour.¹³ Similarly, in New Zealand about 97% of vehicle fires from 1995 to 2003 involved only one vehicle, and a detailed report on United Kingdom vehicle fire statistics from 1994 to 2005 states that about 99% of vehicle fires do not spread to adjoining vehicles.^{12,14}

There have been instances of vehicle fires in parking structures spreading to more than three vehicles. A fire incident in which about 1300 vehicles burned completely in an open multistory parking structure occurred in Liverpool, UK, on

December 31, 2017, and there have been a few other fire incidents involving the burning of three to seven cars.^{12,15} However, the available statistics indicate that such incidents are rare in parking structures and correspond to a very small probability of occurrence. Therefore, vehicle fire scenarios involving one to three vehicles make up the majority of possible vehicle fire scenarios in parking structures.

Evolution of fire temperatures

Temperature evolution during a vehicle fire can vary significantly and has been studied both experimentally and numerically. One such experimental study was conducted by Mangs and Keski-Rahkonen.¹⁶ Three full-scale experiments were conducted on individual passenger cars equipped with standard service accessories and 0.03 m³ (30 L [7.9 gal.]) of gasoline in each fuel tank. Fire was ignited under the engine compartment or in the passenger cabin using a heptane tray. In the first test, the ventilation conditions of the car were varied by keeping the left door 100 mm (3.9 in.) ajar with the window completely open and the right door window 50 mm (2.0 in.) open. In the second and third tests, all doors were kept closed along with one completely open window and three windows open 50 mm (2.0 in.). The vehicle fire behavior was defined by measuring the rate of heat release, mass loss, smoke production rate, heat flux, and temperatures above and inside the car. In all three tests, a peak rate of heat release of 2 MW (6.8 × 10⁶ BTU/hr) and a peak temperature of 1000°C (1832°F) was measured, and a rapid decrease in temperature and rate of heat release was observed after 40 minutes of burning.

In a second study, Mangs and Keski-Rahkonen¹⁷ further used the data generated from their experimental study to define vehicle fires using parametric rate-of-heat-release curves and Alpert's equations.¹⁸ Parametric rate-of-heat-release curves were generated by superimposing one Boltzman and three symmetrical Gaussian curves on the measured rate-of-heat-release curves from the fire tests. The vehicle fire was idealized using two parametric rate-of-heat-release curves, and temperatures were predicted at a given height and distance from the fire plume using Alpert's equations. The predicted temperatures were compared with the corresponding measured temperatures from fire tests and a good correlation between the two was reported by Mangs and Keski-Rahkonen.¹⁷

Another detailed study on closed parking structures was conducted by the European Coal and Steel Community, the results of which were reported by Franssen et al.¹⁹ As part of this study, a total of nine fire tests were conducted (five involved one car burning and four involved two cars burning) on passenger cars to study the rate of heat release, mass loss, and evolution of temperatures in closed parking structures. The conditions of a closed parking structure were simulated for fire tests using an enclosure of 5 × 5 m (16.4 × 16.4 ft) with a height varying from 2.3 to 2.6 m (7.5 to 8.5 ft) and a calorimetric hood on top of the enclosure. All tested cars were equipped with standard accessories and a two-thirds full fuel tank for the first eight tests. In the ninth fire test (involving two cars), the fuel tank of the car

set on fire was one-quarter full and the fuel tank of the adjacent car in the enclosure was empty to limit the resulting rate of heat release under the testing limit of the calorimetric hood. The cars in the first seven tests were ignited using 0.0015 m³ (1.5 L [0.40 gal.]) of gasoline under the left front seat, and the cars in the last two tests were ignited with 0.001 m³ (1.0 L [0.26 gal.]) of gasoline under the gear box. All of the car doors were kept closed with the left windows completely open and the right windows half open for the cars set on fire. However, all doors and windows were kept closed for the adjacent cars not set on fire in the fire tests involving two cars.

A maximum rate of heat release of 10 MW (34.1 × 10⁶ BTU/hr) and maximum fire temperature of 1348°C (2458°F) were measured for the fifth fire test, which involved two cars with two-thirds-full gas tanks. Based on the results of this study, a single-vehicle rate-of-heat-release curve was proposed with a peak rate of heat release of 8.3 MW (28.3 × 10⁶ BTU/hr), 70-minute fire duration, and total fire load of 6.8 GJ (6.4 × 10⁶ BTU) to be representative of the fire scenario involving only one vehicle. For the fire scenario involving multiple vehicles, a similar rate-of-heat-release curve was proposed for subsequent vehicles catching fire. Wave propagation theory was also proposed for scenarios in which fire propagates from one vehicle to an adjacent vehicle every 12 minutes. To get the resulting rate-of-heat-release curve in multiple-vehicle fire scenarios using this approach, the proposed rate-of-heat-release curve for a single vehicle is superimposed with the proposed subsequent vehicle rate-of-heat-release curve at 12-minute intervals, and the resulting area under the superimposed curves represents the final resulting rate-of-heat-release curve for the multiple-vehicle fire. Several numerical studies were performed by Franssen et al.¹⁹ using the proposed rate-of-heat-release curves and wave propagation theory to demonstrate that steel structures do not require high fire resistance in parking structures.

To further develop this assessment, Joyeux et al.¹³ conducted full-scale fire tests in open and closed parking structures. The open parking structure was designed to hold 48 parking bays and measured 32 × 15 × 3 m (105 × 49 × 10 ft). The closed parking structure was smaller, measuring 15 × 10 × 2.4 m (49 × 33 × 7.9 ft). A total of three fire tests were conducted in the open parking structure to study temperature evolution, structural response, and fire propagation. The first two tests involved three cars, with the middle car set on fire. In the third test, two cars were parked in front of each other and then one was set on fire to study fire propagation. In the closed parking structure, two tests were conducted, each involving four passenger cars: three cars in a row and one car behind the middle car. The middle car was set on fire in both tests, and forced ventilation was set up to make these tests relevant to larger parking structures. Based on the results of this study, it was concluded that vehicle fires in parking structures are localized in nature and that smoke is a greater concern in closed parking structures than temperature-induced structural fire damage. Therefore, fire does not pose a significant threat to the overall structural safety of parking structures.

A more recent experimental study was performed by Li et al.²⁰ in which two 2008 four-door sedans were tested side by side in reverse directions to study the evolution of fire temperatures and fire propagation. The fire test was conducted in a room measuring 40 × 12.87 m (131 × 42.22 ft) with a height of 12.0 m (39.4 ft). One car was set on fire using a sponge dipped in gasoline, and the temperature evolution inside and outside of the car was measured using 34 thermocouples. It took only 20 minutes for the fire to propagate to the adjacent car, and the fire reached its fully developed stage, attaining a peak temperature of 900°C (1652°F) inside the car, at 29 minutes. The decay of the fire temperatures started at 35 minutes, and the fire was extinguished at that point to stop the test. Based on the results, Li et al.²⁰ concluded that fire spreads to adjacent vehicles faster through the roof than through the bottom compartment of the car. More studies on the evolution of fire temperatures and simulation of fire spread in multiple-vehicle fire scenarios can be found in the literature.^{12,21–23}

Location of vehicle fire

Because vehicle fires are by nature localized, the location of the burning vehicle or vehicles relative to structural members plays a key role in determining the impact of fire on structural stability. There are limited studies in the literature that focus on predicting the specific location of vehicle fires in a parking structure; therefore, most studies address worst-case fire scenarios only. Based on the literature, Haremza et al.²⁴ identified the following five critical fire scenarios in parking structures:

- one car burning under the midspan of a beam
- two cars burning, one on each side of a column
- seven cars burning in a row near beam supports and columns
- four cars surrounding one column near beam supports
- three cars parked side by side near beam supports and columns

Bayreuther and Pessiki²⁵ also provide a comprehensive study on determining the impact of location on vehicle fire severity.

Rational approach for fire-resistance evaluation

The fire resistance of double-tee slabs can be evaluated through the proposed rational approach, and this analysis can be carried out through a numerical model using any FEA-based software.

Analysis procedure

Figure 2 shows the generic procedure for a proposed rational approach to evaluate the fire resistance of double-tee slabs. This procedure can be applied to fire resistance analysis

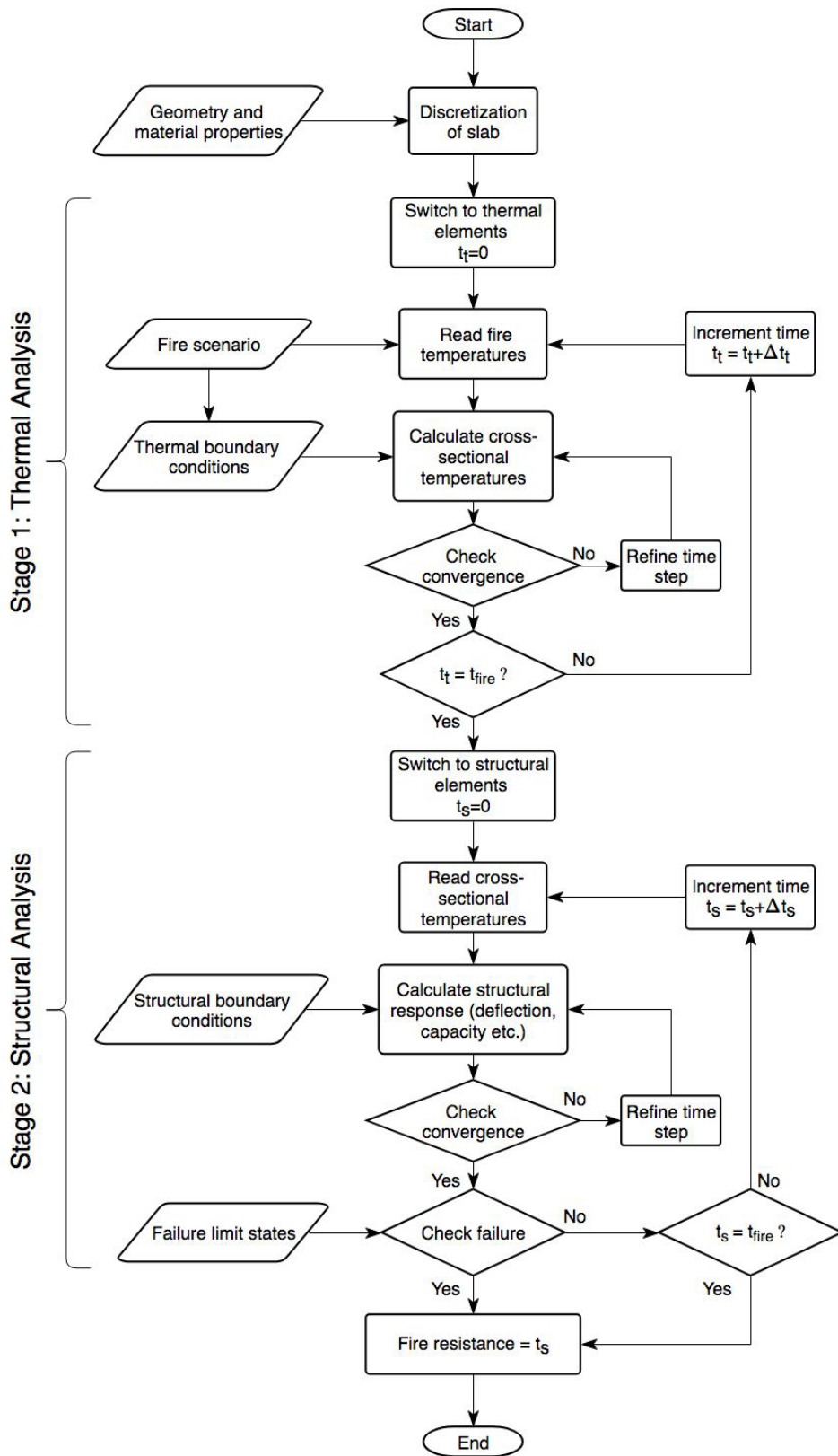


Figure 2. Flowchart illustrating the steps in the rational fire-resistance analysis of double-tee slabs. Note: t_{fire} = total duration of fire exposure; t_s = incremental time in structural analysis; t_t = incremental time in thermal analysis; Δt_s = time increment during structural analysis; Δt_t = time increment during thermal analysis.

in incremental time steps from the start of fire exposure to failure of the slab, or until the end of fire exposure t_{fire} if no failure is observed. The analysis is carried out in two stages: thermal analysis (stage 1) and structural analysis (stage 2). For the analysis, the given geometry of the slab is discretized with two sets of elements, one to simulate the thermal response and the other to simulate the corresponding structural response. The thermal analysis elements are assigned temperature-dependent thermal properties in the thermal domain, and the structural analysis elements are assigned temperature-dependent mechanical properties in the structural domain.

In stage 1 of the analysis, the thermal analysis elements are used to calculate cross-sectional temperatures within a slab in incremental time steps t_i under the specified fire exposure and applied thermal boundary conditions for the complete fire exposure duration. The fire scenario is input in terms of the number of vehicles involved in the fire, temperature-time history, and the location of the fire relative to structural members. Based on the vehicle fire scenario and the desired service conditions of the slab, thermal boundary conditions are specified to define fire-exposed surfaces, the location of the fire, the number of vehicles on fire, heat transfer coefficients, and the initial temperature conditions in the FEA model. If the fire temperatures and boundary conditions are known, a set of heat transfer equations are solved within the program at every time step to evaluate sectional temperatures along the slab length. These equations require nonlinear algorithms to be solved, and convergence problems can occur in reaching a solution due to the varying material properties at elevated temperatures. When this happens, the time step is refined by reducing the incremental time step and the analysis is repeated. This procedure is followed in incremental time steps for the entire duration of fire exposure.

After the thermal analysis, the thermal elements are changed to compatible structural elements in stage 2 of the analysis and the cross-sectional temperature results from the thermal analysis are used as input for the structural analysis. Other input parameters include structural boundary conditions and failure limit states. At every time step of the structural analysis t_s , structural response parameters are generated by solving mechanics-based equations. The resulting output parameters are nodal deflections and element stresses. The response parameters from the thermal and structural analyses are used to evaluate failure limit states at the end of every time step. If one or more limit state is exceeded, failure is said to occur in the slab, and the total duration of fire exposure to reach that time step is taken as the fire resistance of the slab. Otherwise, analysis continues in incremental time steps for the duration of the fire exposure. ANSYS FEA software is used for the analysis, the details of which are presented in the following sections.

Discretization of the double-tee slab

For the thermal and structural analyses, the double-tee slab is discretized into two sets of elements. The elements need-

ed to facilitate thermal analysis are SOLID70, LINK33, and SURF152. SOLID70 is a three-dimensional eight-node element capable of modeling thermal conduction and is used to simulate heat transfer (conduction) within concrete. The element has one degree of freedom at each node (temperature) and can simulate steady state or transient thermal analysis. LINK33 is a two-node uniaxial line element with one degree of freedom at each node (temperature), and it can simulate both steady and transient thermal analysis as well. LINK33 is used to model thermal conduction within prestressed strands. SURF152 is a four-node surface element capable of simulating heat transfer via conduction, convection, and radiation, and is overlaid on the fire-exposed surfaces of the double-tee slab to simulate heat transfer between the fire zone and the slab. To simulate convection and radiation heat transfer, an additional node is assigned to SURF152 elements away from base element geometry, which represents the source of heat. Heat flux is then calculated based on the geometry of the extra node relative to the base element to simulate convection and radiation heat transfer.

To simulate the structural response, SOLID70 is changed to SOLID65 following thermal analysis, and similarly, LINK33 is changed to LINK180 and SURF152 to SURF154. The SOLID65 element is an eight-node element that is used to simulate the cracking and crushing of concrete in three orthogonal directions using the Willam-Warnke failure envelope. The SOLID65 element has three translational degrees of freedom at each node and can account for nonlinear material models as well. LINK180 elements are uniaxial two-node elements with three translational degrees of freedom at each node and can simulate nonlinear material models with initial stress or strain conditions. LINK180 elements are used to simulate the effect of prestress and compression or tension within prestressing strands. SURF154 elements are used for the application of surface loads on the discretized slab. **Figure 3** shows a typical cross section of a double-tee slab discretized into various elements.

Material properties at elevated temperatures

Temperature-dependent thermal and mechanical material property relations are provided as input to the FEA model to simulate the response of structural members under fire exposure. The thermal and mechanical property relations for concrete and steel were considered to vary with temperature according to Eurocode 2.²⁶ In the thermal analysis, density, thermal conductivity, and specific heat of concrete and steel are allowed to vary with temperature, whereas in the structural analysis, elastic modulus, stress-strain constitutive model, and thermal strain are considered to vary with temperature as per Eurocode 2 recommendations. During the structural analysis, concrete was assigned a multilinear, temperature-dependent elastic modulus along with a temperature-dependent nonmetal plasticity constitutive model, whereas prestressing strands were assigned a temperature-dependent multilinear kinematic hardening constitutive model.

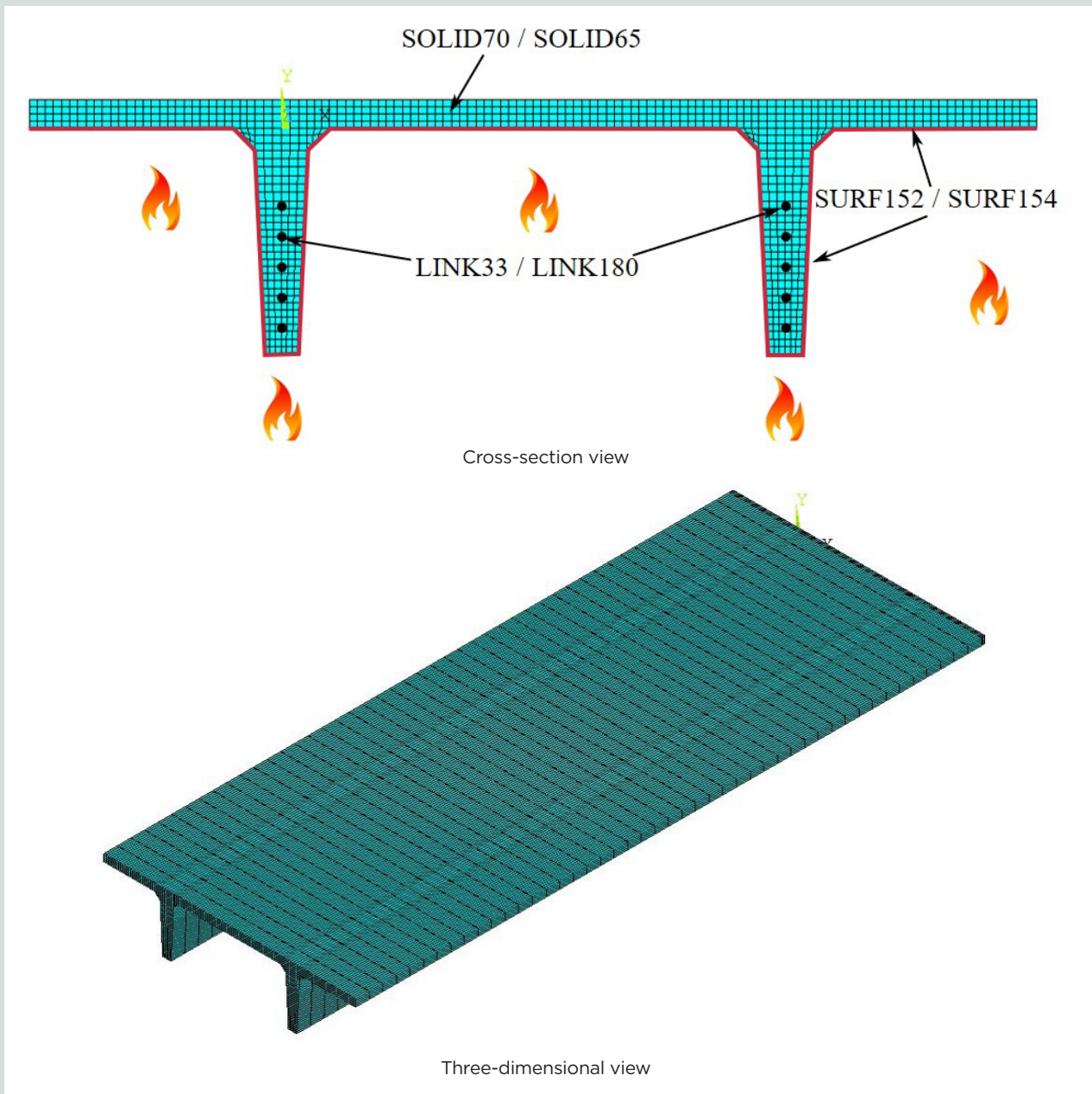


Figure 3. Discretization of a typical double-tee slab for finite element analysis

Also, due to the rapid burning that can occur during vehicle fires, the convective heat transfer between the fire and the exposed surface of the slab is significantly higher than in building fires. A convective heat transfer coefficient was assigned to the SURF152 elements on the slab face exposed to the fire to account for the effects of the vehicle fire. Eurocode 1²⁷ specifies a value of 50 W/(m²-K) [8.8 BTU/(hr-ft²-°F)] for the convection heat transfer coefficient for hydrocarbon fires, and 25 W/(m²-K) [4.4 BTU/(hr-ft²-°F)] for standard building fires. However, due to a lack of specific experimental data for vehicle fires, a slightly conservative convective heat transfer coefficient of 45 W/(m²-K) [7.9 BTU/(hr-ft²-°F)] was selected for vehicle fire scenarios in this study. Different convection

heat transfer coefficients can be input if the exact value of the coefficient is known.

Cracking and crushing of concrete

Concrete loses significant stiffness from sustained cracking and crushing under high-temperature fire exposure, and this degradation plays a key role in defining the fire response of concrete structural members. Therefore, cracking and crushing of concrete at elevated temperatures is simulated in SOLID65 concrete elements using the Willam-Warnke failure envelope. This failure envelope has been successfully applied by researchers for other concrete structural members under

fire exposure and is suitable for modeling the response of concrete at elevated temperatures.^{28,29} The failure criterion for a multiaxial stress state of concrete is expressed as:

$$\frac{F}{f_{c\theta_e}} - S \geq 0 \quad (1)$$

where

F = function of principal stress state

$f_{c\theta_e}$ = compressive strength of concrete at element temperature θ_e

S = continuous failure surface

Detailed equations for evaluating F and S can be found in the literature.²⁸ If an element satisfies the failure criterion of Eq. (1), either cracking or crushing of the element can occur based on the dominating principal stress state. In all such cases, the crushing of the element is simulated by reducing the stiffness of the element to a negligible value, and cracking is simulated by introducing a plane of weakness (cracking plane) perpendicular to the corresponding principal stress. The stiffness of the element is reduced along the cracking plane by using open and closed crack coefficients in the FEA model. Typical values of these parameters range between 0 and 1, with 0 representing complete loss of shear transfer (smooth crack) and 1 representing no loss of shear transfer (rough crack). Based on preliminary studies, these parameters were assigned a value of 0.2 and 0.7, respectively.

Failure limit states

Double-tee slabs can fail by one or more failure limit states. Failure at the insulation limit state occurs when the average temperature increase on the unexposed surface of the slab exceeds 139°C (282°F).¹ Alternatively, when the slab is not able to maintain the applied loading during fire exposure, it is considered a stability failure. Under the prescriptive approach to fire-resistance evaluation, stability failure is assessed using the temperature-based limit state only; that is, stability failure occurs when the temperature in the strands surpasses the critical temperature (427°C [801°F]).¹ However, this is not a realistic representation of the failure that occurs through an intricate thermomechanical response of the slab. Therefore, as part of the rational approach, stability failure is assessed by three different strength-based limit states, namely shear, moment, and deflection limit states, which account for the intricate thermomechanical response of the slab.

The reduced moment capacity M_{nt} at time t under fire exposure is evaluated by combining temperatures from the FEA with the moment capacity equation from the *PCI Design Handbook: Precast and Prestressed Concrete*⁹ as:

$$M_{nt} = A_{ps} f_{ps\theta_t} \left(d - \frac{a_t}{2} \right)$$

$$f_{ps\theta_t} = f_{ps\theta_t} \left(1 - \frac{0.5 A_{ps} f_{ps\theta_t}}{b d f_{c\theta_t}} \right)$$

$$a_t = \frac{A_{ps} f_{ps\theta_t}}{0.85 f_{c\theta_t} b}$$

where

A_{ps} = area of prestressing steel

$f_{ps\theta_t}$ = actual stress in prestressing strands at average strand temperature θ_s corresponding to time t

d = effective depth of slab

a_t = depth of equivalent rectangular stress block at time t

$f_{ps\theta_t}$ = ultimate stress in prestressing strands at average strand temperature θ_s corresponding to time t

b = width of slab

$f_{c\theta_t}$ = compressive strength of concrete evaluated at average temperature in zone of rectangular stress block θ_c at time t

Similarly, the reduced shear capacity V_{nt} of a slab at time t under fire exposure is evaluated by expanding the room-temperature shear capacity equation given in the *PCI Design Handbook*⁹ as:

$$V_{nt} = \left(0.6 \sqrt{f_{c\theta_t}} + 700 \frac{V_u d}{M_u} \right) b_w d \leq 5 \sqrt{f_{c\theta_t}} b_w d$$

and

$$V_{nt} \geq 2 \sqrt{f_{c\theta_t}} b_w d$$

where

$f_{c\theta_t}$ = compressive strength of concrete evaluated at average cross-sectional concrete temperature θ_a at time t

V_u = applied shear load under fire conditions

M_u = applied moment under fire conditions

b_w = thickness of web

Failure under the moment or shear limit state occurs when the reduced moment or shear capacity is less than the applied moment or shear during fire exposure.

Failure occurs at the deflection limit state when the maximum deflection in the slab exceeds $L/20$ at any fire exposure time or the rate of deflection exceeds $L^2/9000d$ (mm/min) after a

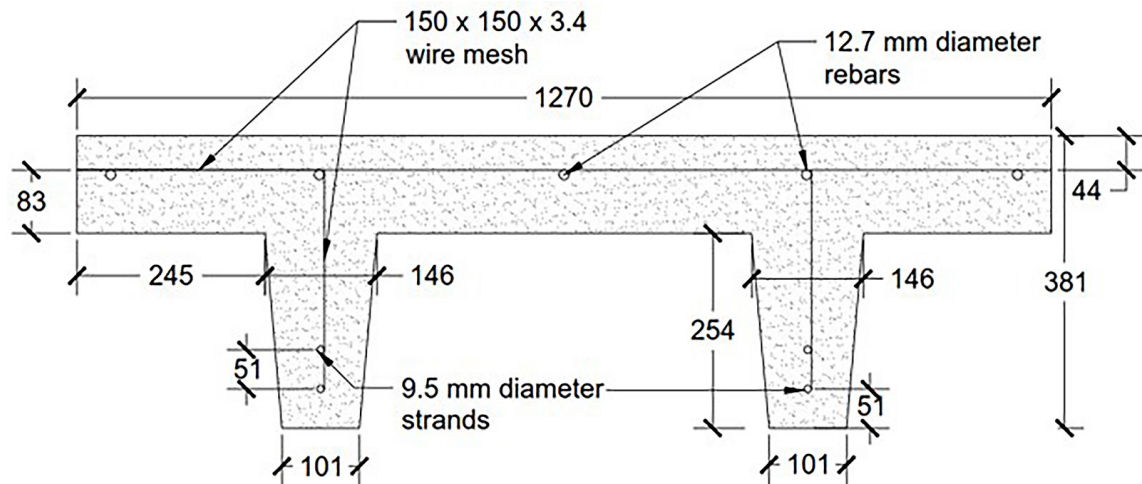


Figure 4. Geometry of the slab selected for validation (DT). Note: All dimensions are in millimeters. 1 mm = 0.0394 in.

maximum deflection of $L/30$ is reached, where L is the length of the slab in millimeters and d is the effective depth of the slab in millimeters.³⁰ This limit state was applied by comparing the predicted deflection output from the FEA at each time step with the previously mentioned deflection limits.

Model validation

The numerical model was validated by comparing thermal and structural response predictions from the model with published data from a fire test on a full-scale double-tee slab exposed to a standard fire.³¹

Selected slab for validation

Selvaggio and Carlson³¹ tested a series of double-tee slabs under standard fire exposure. In this study, one of the tested slabs from the previous study was selected for validation and designated slab DT. The dimensions of slab DT were $5.48 \times 1.27 \times 0.38$ m ($18.0 \times 4.17 \times 1.25$ ft). Each tee was fabricated with two layers of 9.5 mm (0.37 in.) diameter strands, and 1.82 m (5.97 ft) long \times 12.7 mm (0.5 in.) diameter reinforcing bars were provided as compression reinforcement in the flange near the supports. Furthermore, welded-wire reinforcement was provided in the top flange primarily for crack control under serviceability conditions. **Figure 4** shows the detailed geometry of slab DT along with the reinforcement. The ultimate strength of the strands was 1723 MPa (250 ksi), and they were tensioned to 1206 MPa (175 ksi), 70% of the ultimate strength, during the fabrication of the tested slab. The slab DT concrete contained calcareous coarse aggregate and had a compressive strength of 38 MPa (5.5 ksi). The tested slab was loaded to 55% of its flexural capacity with axially restrained supports and was tested under standard fire expo-

sure for four hours. The axial displacement of the slab was constrained to 19 mm (0.75 in.) using vertical plates at the ends. The fire response of the double-tee slab was measured in terms of cross-sectional temperatures and midspan deflection.

Analysis details

The proposed numerical model was applied to analyze slab DT under identical loading and boundary conditions to the fire test.³¹ Due to symmetry in loading, geometry, and boundary conditions, a quarter of the slab was analyzed for the FEA model. The symmetric boundary condition was implemented by constraining the out-of-plane displacement and rotational degree of freedom at the plane of symmetry. For simplicity, the welded-wire reinforcement was not considered in the numerical model because it did not contribute significantly to the structural response of the slab. These simplifications significantly reduced the number of elements required to discretize the slab and led to faster analysis with high computational efficiency. The analysis was carried out at two-minute time increments, and the fire response was traced until failure or completion of the four-hour fire exposure.

Thermal response

Figure 5 compares the predicted and measured temperatures at various cross-sectional depths of slab DT. It shows that strand temperatures were underpredicted by the model during the first 110 minutes of fire exposure and then overpredicted for both the lower and upper strands for the remaining fire duration. Alternatively, the unexposed face temperatures were predicted with relatively better accuracy throughout the four hours of fire exposure. Some of the differences between the predicted and measured temperatures may be due to the con-

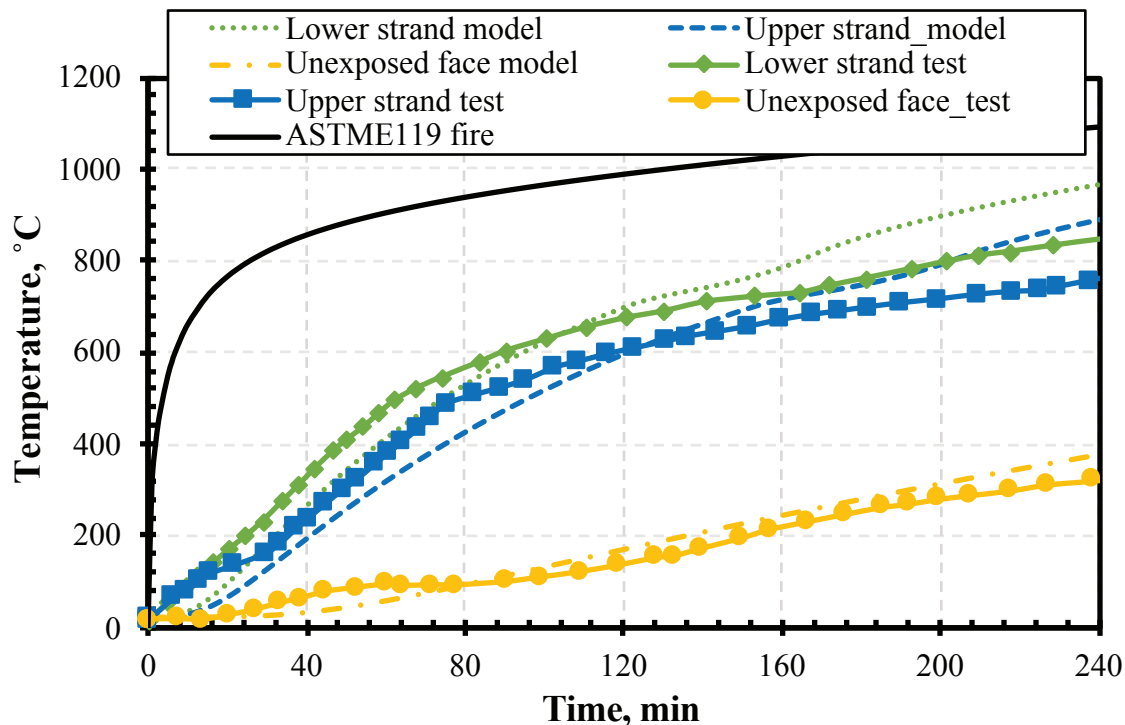


Figure 5. Comparison of predicted and measured temperatures for the slab selected for validation (DT). Note: $^{\circ}\text{C} = (^{\circ}\text{F} - 32)/1.8$.

siderable variation between the desired ASTM fire exposure and the actual furnace temperatures in the fire test by Selvaggio and Carlson³¹ that were affected by the large size of the furnace and other experimental constraints. Therefore, unlike the numerical analysis, slab DT was exposed to relatively nonuniform fire conditions in the fire test. Furthermore, the reported sectional temperatures at a given depth from the testing are the average of all of the thermocouples (placed along the length of the slab) at that depth to minimize the impact of any experimental errors in the recorded temperatures. Therefore, the variations between the predicted and measured temperatures are due to the nonuniform nature of the experimental results previously noted, as well as slight differences between the actual and specified material properties of concrete. However, the overall temperature progression trends were captured well for slab DT, and therefore the developed numerical model is deemed to satisfactorily trace the thermal response of double-tee slabs.

Structural response

Figure 6 compares the predicted and measured midspan deflections for slab DT. The midspan deflection of the tested slab increased suddenly in the first 15 minutes of fire exposure, which was attributed to the loss of prestress in strands due to thermal expansion. From 15 to 200 minutes, deflection

increased at a moderate pace due to the combined effects of material property degradation, thermal expansion, and axial restraint. At 200 minutes, the strand temperatures surpassed 800°C (1472°F), causing significant strength and stiffness degradation in the strands and leading to an increased rate of deflection. This trend in deflection was captured well by the model, and overall there was good correlation between predicted and measured deflections. Therefore, the developed numerical model captured the deflection response of slab DT with reasonable accuracy and can be used to predict the thermomechanical response of double-tee slabs.

Case study

A case study was analyzed to illustrate the applicability of the proposed rational approach to evaluate the fire resistance of typical double-tee slabs in parking structures.

Selection of case study slabs

The typical spans of double-tee slabs in parking structures range from 12.2 to 27.4 m (40 to 90 ft).⁹ A 12DT32 double-tee section (a typical double-tee cross section according to the *PCI Design Handbook*⁹) with a span of 17.7 m (58.1 ft) was selected for the case study. Double-tee slabs typically have variable topping thickness (pretopped or

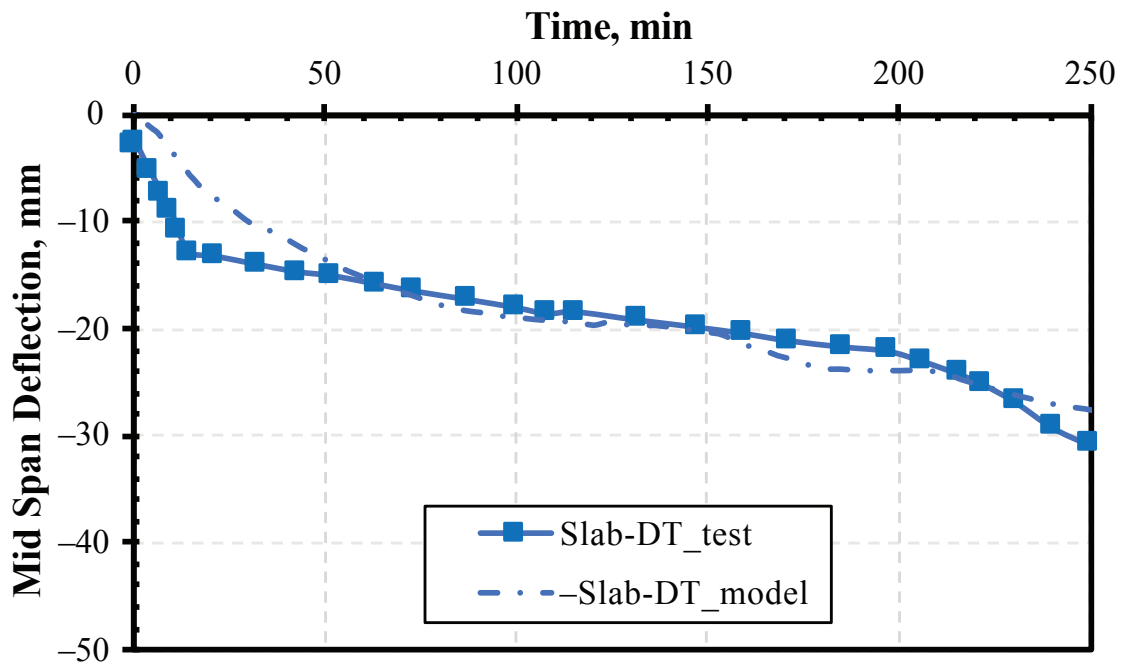


Figure 6. Comparison of predicted and measured midspan deflections for the slab selected for validation (DT). Note: 1 mm = 0.0394 in.

constructed in place) in parking structures to protect the slab surface from wear and tear, for leveling and finishing purposes, and to provide additional structural strength from composite action between the topping and the slab. The most common topping thickness of 51 mm (2 in.) was used for the selected double-tee slab (12DT32+2) to determine the effects of the topping on the fire resistance of the slab.

Table 1 provides detailed information about these two slabs

(12DT32 and 12DT32+2), and **Fig. 7** shows their cross-sectional geometry.

Selection of vehicle fire scenario

As previously discussed, vehicle fire scenarios involving one to three vehicles make up nearly 96% of all possible fire scenarios in parking structures. Therefore, the full-scale experi-

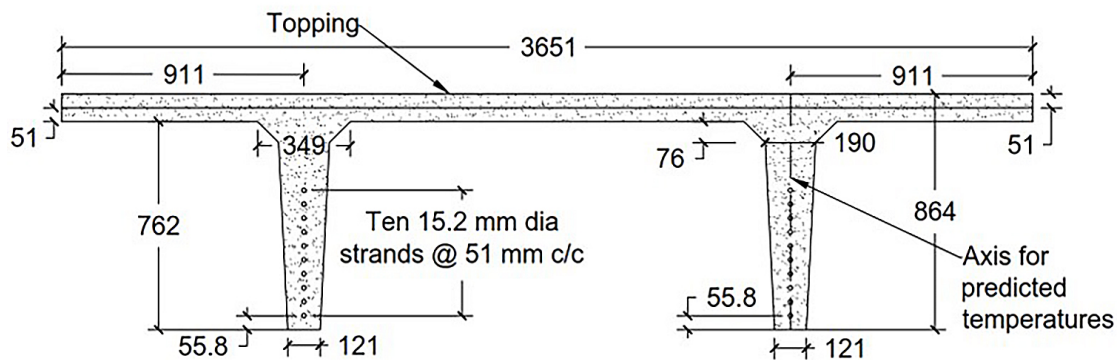


Figure 7. Geometry of 12DT32+2. Note: 12DT32 has the same geometry as 12DT32+2 without the 51 mm topping and with eight strands in each tee. Note: All dimensions are in millimeters. c/c = center-to-center; dia = diameter. 1 mm = 0.0394 in.

Table 1. Input parameters for rational fire-resistance evaluation of the selected case study double-tee slabs

Category	Parameter	12DT32	12DT32+2
Geometry	PCI designation	12DT32-89S	12DT32+2-109S
	Cross section	See Fig. 7	See Fig. 7
	Concrete cover, mm	55.8	55.8
	Span, m	17.7	18.3
	Prestressing strands	Eight 15.2 mm diameter strands	Ten 15.2 mm diameter strands
Material properties	Concrete strength, MPa	41.4	41.4
	Aggregate type	Calcareous	Calcareous
	Strand strength, MPa	1860	1860
	Prestress in strands, MPa	1302	1302
	High-temperature properties	Eurocode 1 and 2	Eurocode 1 and 2
Fire scenario	Number of vehicles	3	3
	Fire temperatures	Parking fire 1 and 2	Parking fire 1 and 2
Thermal analysis	Boundary conditions	Three-sided exposure	Three-sided exposure
	Convective heat transfer coefficient, W/m ² /K	45	45
Structural analysis	Support	Simply supported	Simply supported
	Vehicle live load, kN/m ²	2.15	2.15
Failure check	Limit states	Insulation, shear, moment, deflection	Insulation, shear, moment, deflection

Note: 1 mm = 0.0394 in.; 1 m = 3.281 ft; 1 MPa = 0.145 ksi; 1 kN/m² = 20.89 lb/ft²; 1 W/(m²K) = 0.1762 BTU/(hr-ft²-°F).

mental study by Zhao and Kruppa³² on vehicle fires was used in the present study to define the vehicle fire scenario. The study by Zhao and Kruppa considered two full-scale vehicle fire scenarios involving three cars in an open parking structure, where a fire was started in the middle vehicle and the evolution of fire temperatures was recorded. Figure 1 shows the measured temperatures from the study, where parking fire 1 represents a slow fire progression and the resulting fire temperatures with a longer burning duration, and parking fire 2 represents a vehicle fire with a rapid rise in fire temperatures and a shorter burning duration. The entire bottom portion of the slab was exposed to the fire (using the temperature-time relationship shown in Fig. 1), instead of selecting a localized fire exposure. This conservative approach was chosen because there can be significant uncertainty associated with predicting the location of a vehicle fire.

Analysis details

These two case-study slabs were analyzed using the previously described procedure. Due to symmetry in loading, geometry, and boundary conditions, a quarter of each slab was analyzed for the 12DT32 and 12DT32+2 FEA models. Both slabs were analyzed under two vehicle fire exposures, parking fire 1 and parking fire 2, as well as the ASTM E119¹ standard fire exposure for comparison purposes. For all case

studies, a combination of dead load and vehicle live load was selected (because vehicles are most likely to be present during fire exposure) to represent realistic loading conditions during fire exposure. A vehicle live load of 2.15 kN/m² (45 lb/ft²) was selected in accordance with ASCE 7,³³ which accounts for the vehicle loading and dynamic effects in a parking structure. Fire-resistance analysis was carried out at two-minute intervals. Table 1 provides a sequential list of the input parameters used for the rational approach analysis.

Thermal response

Figure 8 shows the progression of cross-sectional temperatures along the vertical axis passing through the strands (Fig. 7) in 12DT32 under vehicle and standard fire exposures (ASTM E119¹ fire). In parking fire 1 (Fig. 8), the fire temperatures increased slowly at first until 40 minutes, and then peak fire temperatures were attained from 40 to 55 minutes, followed by a decay phase. Due to the slow rise in fire temperatures until 40 minutes of fire exposure, cross-sectional temperatures within the slab were almost unaffected during the initial 30 minutes of fire exposure and then increased at a moderate pace for all depths. The peak temperature in bottom prestressing strands was 250°C (482°F), and decay in strand temperature started at a time lag of about 30 minutes from the beginning of the fire decay phase. Temperatures at the inner

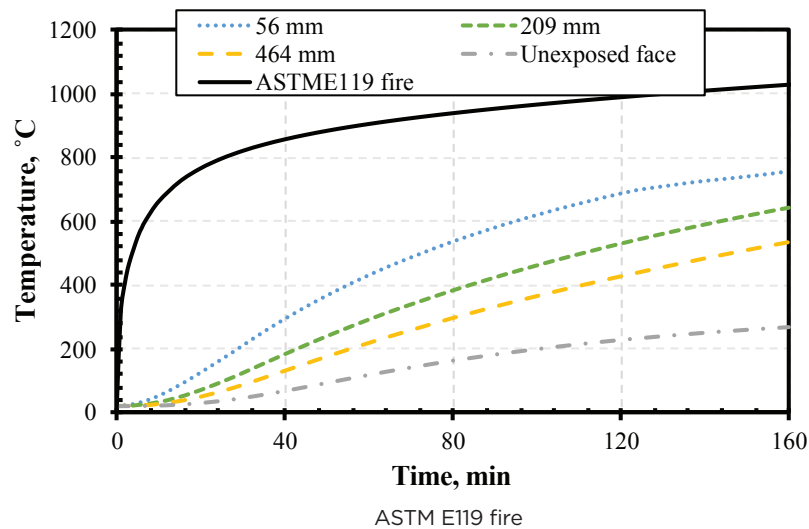
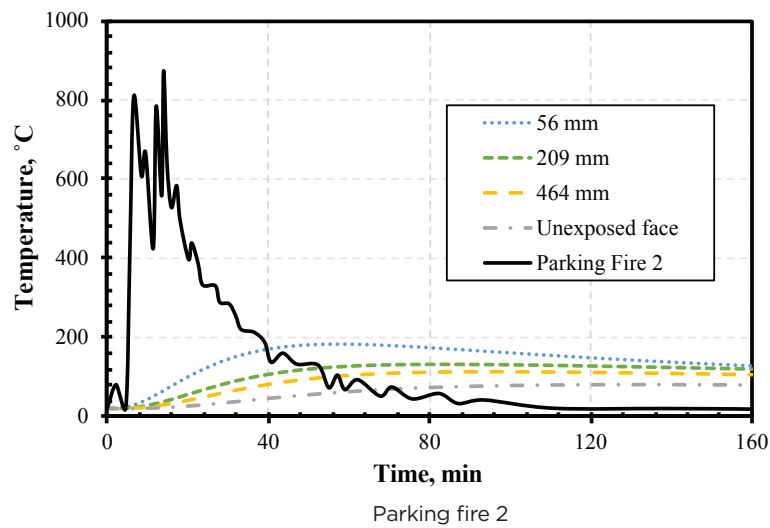
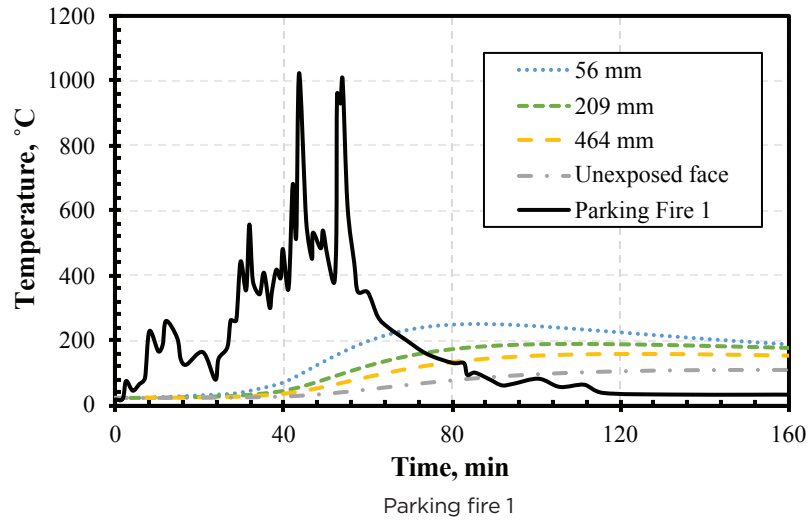
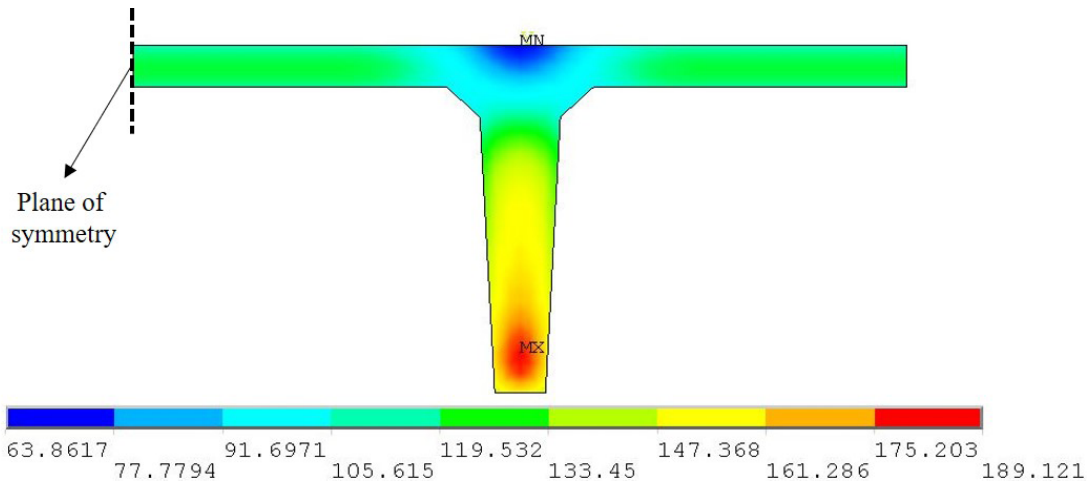
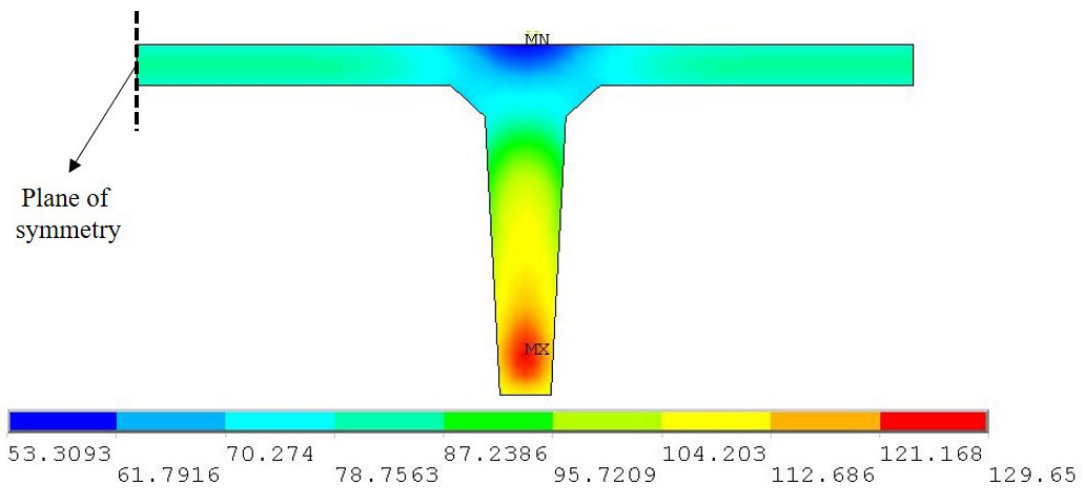


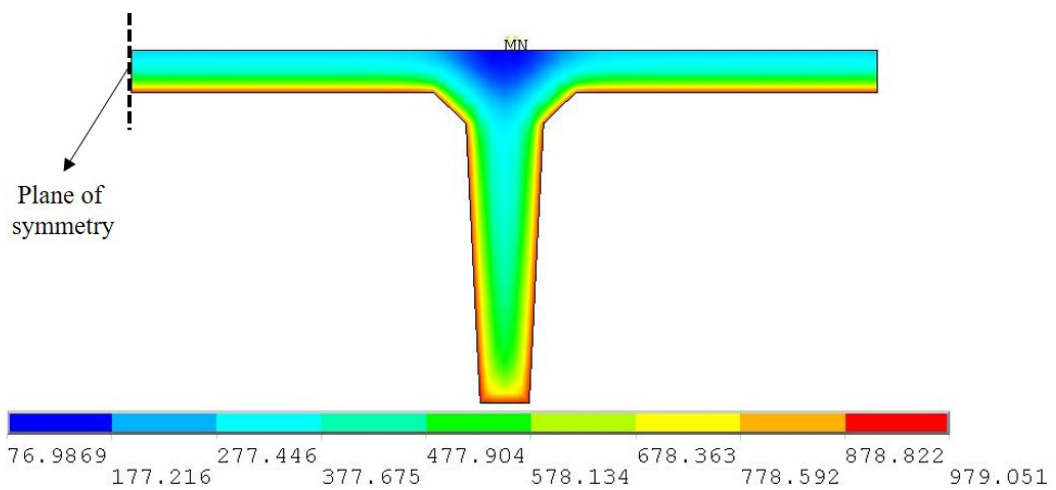
Figure 8. Predicted thermal response for 12DT32 under different fire exposures at increasing depths from the bottom face of the tee along the vertical axis passing through the strands. Note: 1 mm = 0.0394 in; °C = (°F - 32)/1.8.



Parking fire 1 at 160 minutes



Parking fire 2 at 160 minutes



ASTM E119 fire at 100 minutes

Figure 9. Cross-sectional temperature contours in 12DT32+2 double-tee slab under different fire exposures. Note: °C = (°F - 32)/1.8.

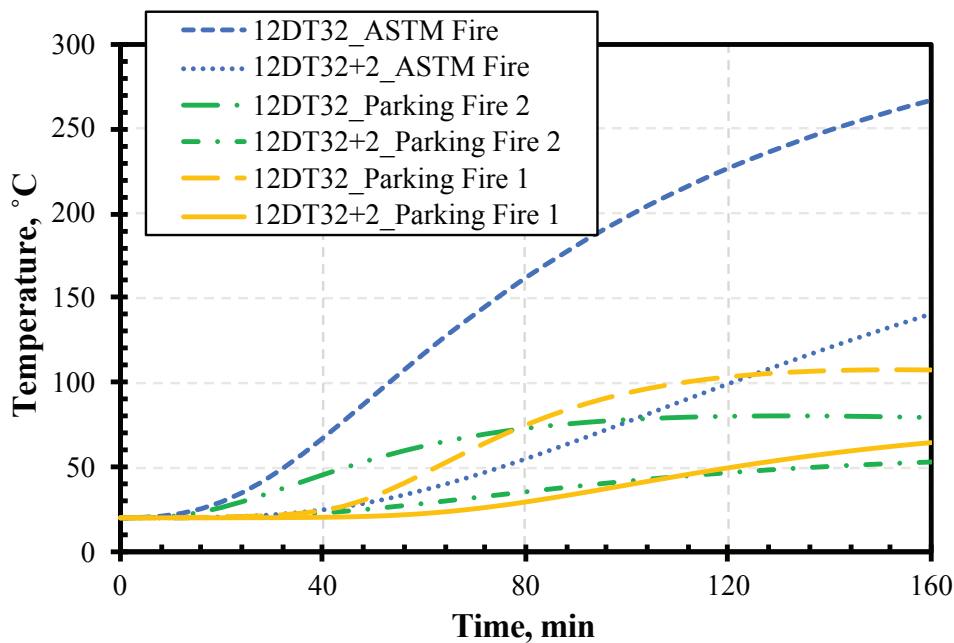


Figure 10. Comparison of predicted unexposed face temperatures for slabs 12DT32 and 12DT32+2. Note: °C = (°F - 32)/1.8.

depths of the slab progressed much more slowly compared with strand temperatures and with greater time lags relative to the fire temperature decay phase due to the high thermal inertia of concrete.

In parking fire 2 (Fig. 8), the fire temperatures increased rapidly and attained peak temperatures within 15 minutes of fire exposure followed by a decay phase. Therefore, unlike parking fire 1, there was a smaller time lag for the increase in cross-sectional temperatures, and temperatures increased at all depths at a moderate pace from the start of the fire exposure. The peak temperature in bottom prestressing strands was well below 200°C (392°F) at a time lag of about 40 minutes from the start of the fire temperature decay phase. This greater time lag in reaching peak temperature was due to rapid heating of the slab in the initial stages of fire exposure, which did not allow ample time to overcome the thermal inertia of concrete. Evolution of sectional temperatures under parking fire 2 was similar to parking fire 1 with the temperatures at the inner depths of the slab progressing more slowly than the strand temperatures and at a greater time lag from the occurrence of the fire decay phase due to the high thermal inertia of concrete.

In the standard fire exposure (Fig. 8), the cross-sectional temperatures continued to increase due to the absence of a decay phase, and bottom strand temperatures reached a maximum of 760°C (1400°F) for 12DT32 and 12DT32+2, which caused the strands to lose about 92% of their strength. However, the

peak cross-sectional temperatures in the concrete and prestressing strands were well below 250°C (482°F) for both vehicle fire exposures in 12DT32 and 12DT32+2, and the strands lost only 8.5% of their strength at this temperature. To demonstrate the differences in progression of sectional temperatures under different fire exposures, temperature contours in the 12DT32+2 double-tee slab under different fire exposures are shown in Fig. 9. Temperature contours are plotted at the time of failure or end of fire exposure, which is 160 minutes for parking fires 1 and 2 and 100 minutes for ASTM fire exposure. It can be clearly seen in Fig. 9 that cross-sectional temperatures are well below 190°C (374°F) under parking fire 1 and below 130°C (266°F) under parking fire 2, whereas sectional temperatures are as high as 979°C (1794°F) under standard ASTM fire exposure. Therefore, using standard fire exposure to represent vehicle fires in parking structures is highly conservative.

It should be noted that the same temperature trends were observed under vehicle and standard fire exposures for 12DT32+2 and 12DT32 double-tee slabs. The only major difference between the temperature progressions in 12DT32 and 12DT32+2 was lower unexposed face temperatures in 12DT32+2 due to greater slab thickness (102 mm [4 in.] in 12DT32+2 compared with 51 mm [2 in.] in 12DT32). **Figure 10** compares the predicted unexposed face temperatures of 12DT32 and 12DT32+2 and shows that the unexposed face temperatures in 12DT32+2 were well below the corresponding 12DT32 values.

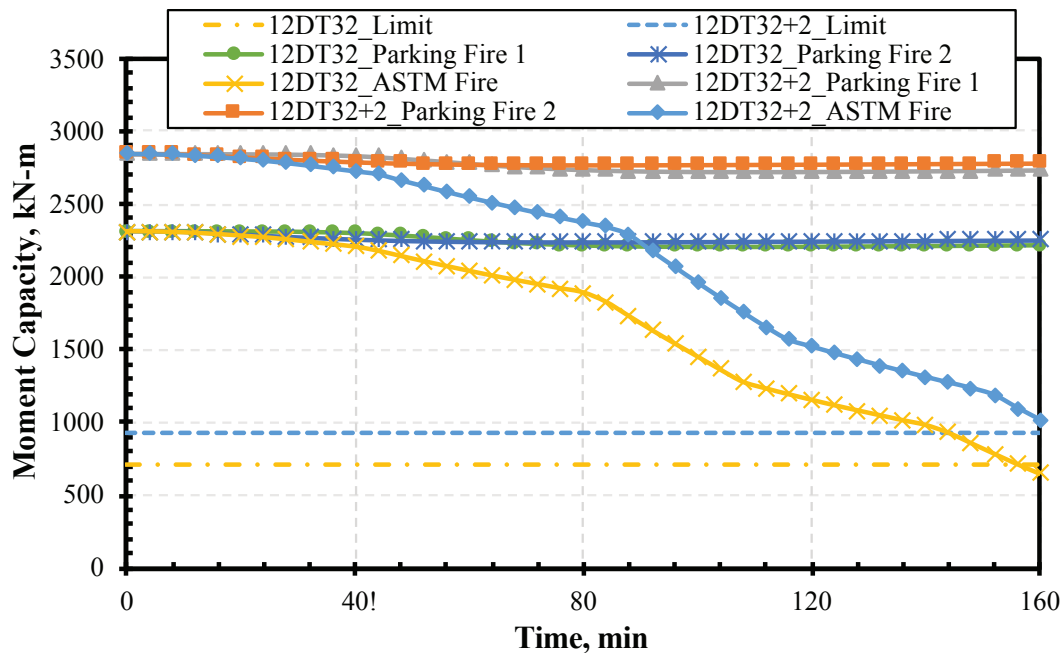


Figure 11. Predicted moment capacity degradation for slabs 12DT32 and 12DT32+2 under different fire exposures. Note: 1 kN-m = 8.85 kip-in.

Structural response

Figures 11 and 12 compare the degradation in moment and shear capacity of the slabs for each fire exposure, and Fig. 11 shows that degradation of moment capacity under both vehicle fire exposures was almost negligible compared with the response under standard fire exposure. In parking fire 2, the moment capacity degradation attained peak value at an earlier fire exposure time than in the parking fire 1 exposure. This was due to the lag in the rise of cross-sectional temperatures in the initial 30 minutes of fire exposure for parking fire 1, as previously explained. However, the extent of degradation in moment capacity for the parking fire 1 exposure was relatively higher than for the parking fire 2 exposure, which was due to higher strand temperatures sustained in the parking fire 1 exposure (Fig. 8). The degradation in shear capacity was almost negligible for both parking fires 1 and 2 exposures and minimal for the standard fire exposure (Fig. 12).

Figure 13 shows the progression of midspan deflections under three fire exposures for the complete duration of fire exposure. Both 12DT32 and 12DT32+2 experienced negligible deflection under the vehicle fire exposures compared with the response under the standard fire exposure. Furthermore, in the vehicle fire scenarios, the effect of the cooling phase can be clearly observed in the structural response (Fig. 11–13), as the capacity degradation and midspan deflections stabilized after attaining peak values and did not reach the limiting criteria. However, for the standard fire exposure, a continuous

degradation of the sectional capacity and an increase in the midspan deflections occurred until ultimate failure was attained. Therefore, it is important in fire-resistance analysis to consider the effects of the cooling or decay phase in realistic fire scenarios.

Failure times and failure modes

Failure of 12DT32 and 12DT32+2 was evaluated using the previously discussed failure limit states. Failure occurred under standard fire exposure only for both 12DT32 and 12DT32+2. Failure of 12DT32+2 occurred when the deflection limit state was exceeded at 100 minutes, while the corresponding failure time in 12DT32 was 69 minutes, but under the insulation limit state. This was primarily due to the smaller flange thickness of 12DT32 (51 mm [2 in.]), which allowed the temperature to rise rapidly on the unexposed face, thus reaching the insulation limit before the deflection limit was reached. Both slabs failed under standard fire exposure only, and no failure occurred under vehicle fire exposure. Furthermore, the progression in cross-sectional temperatures and capacity degradation under vehicle fire exposure was minimal compared with standard fire exposure (Fig. 8–13), which confirms the overly conservative nature of the prescriptive approach, which can lead to costly designs.

Double-tee slab 12DT32+2 failed under deflection limit state; its cracking and crushing patterns are provided in Fig. 14. These profiles are created at the time of failure or end of

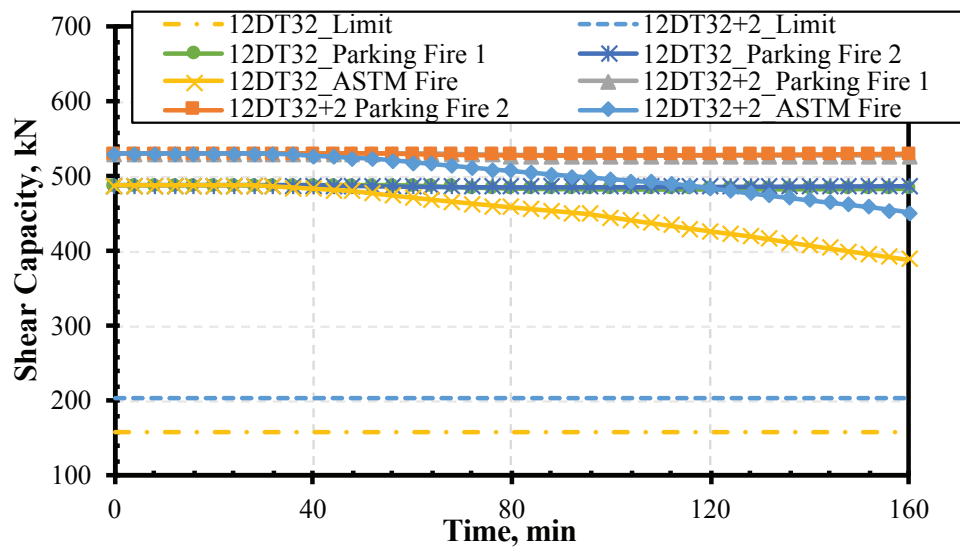


Figure 12. Predicted shear capacity degradation for slabs 12DT32 and 12DT32+2 under different fire exposures. Note: 1 kN = 0.2248 kip.

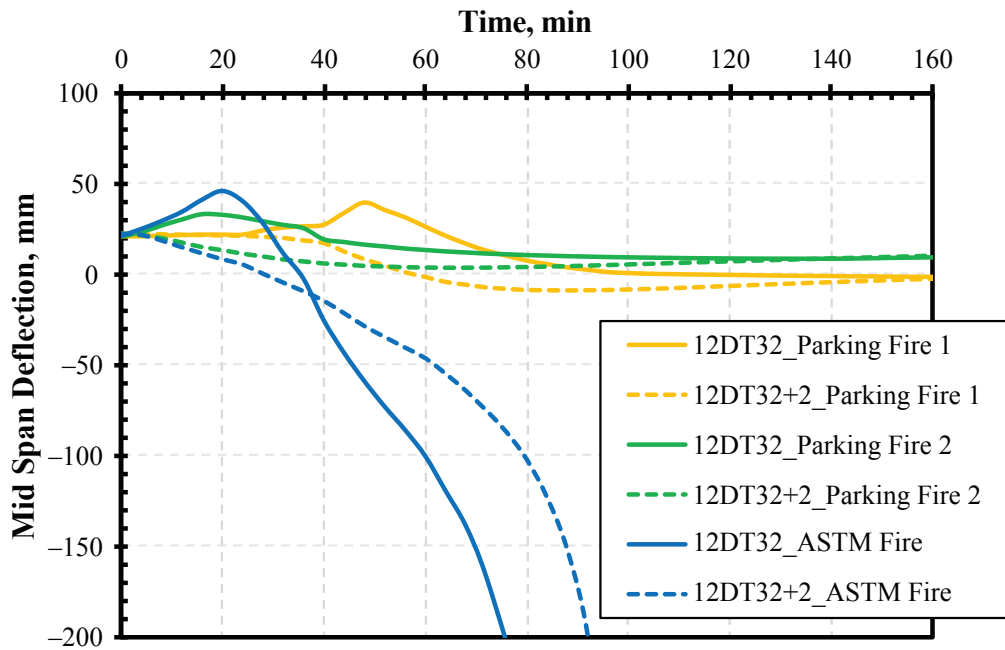


Figure 13. Predicted deflection response for slabs 12DT32 and 12DT32+2 under different fire exposures. Note: 1 mm = 0.0394 in.

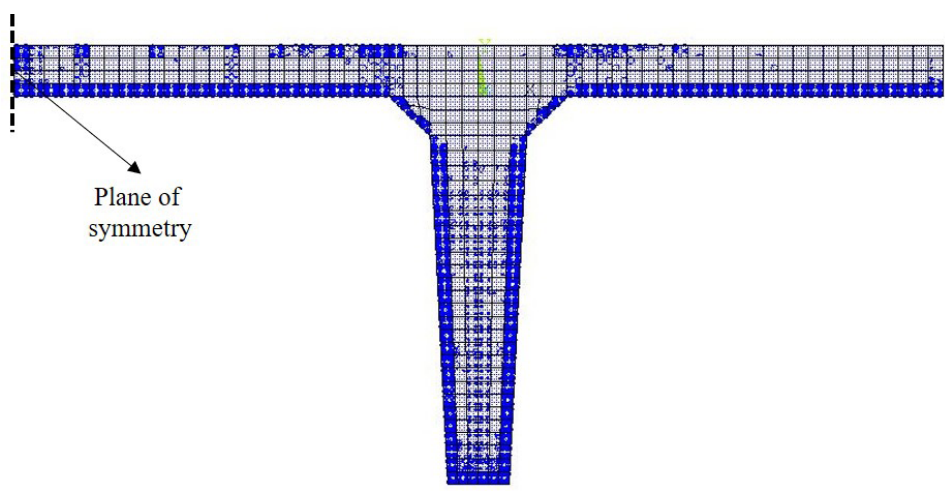
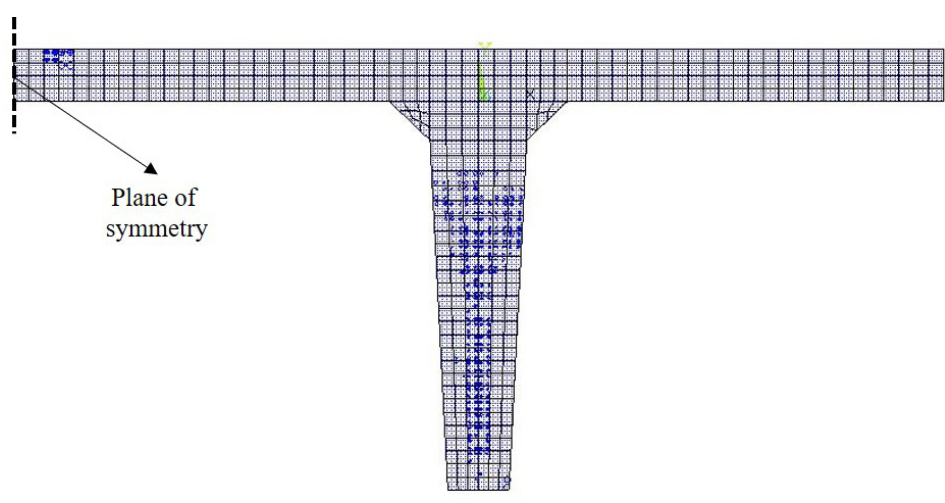
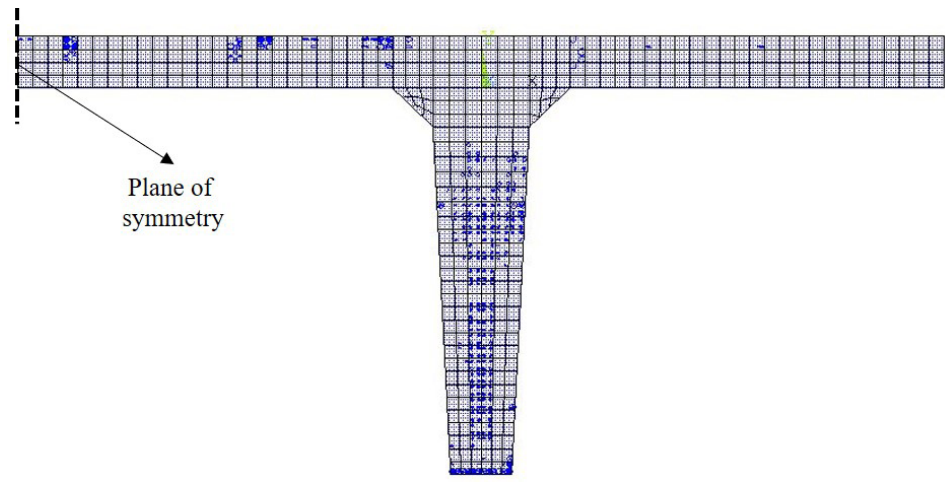


Figure 14. Cracking and crushing profile in cross-section of 12DT32+2 double-tee slab under different fire exposures.

analysis, which is 160 minutes for parking fires 1 and 2 and 100 minutes for ASTM fire exposure. It can be seen from Fig. 14 that most of the cracking is limited to the vicinity of strands in the tee for both parking fires 1 and 2, and only minor cracking and crushing is observed in the flange. On the other hand, significant cracking and crushing occurred on the exposed face of the double-tee under ASTM fire exposure due to significantly higher temperatures experienced under ASTM fire exposure at the exposed surface (Fig. 9). Unlike parking fires 1 and 2, cracks on the exposed fire surface propagate across the flange and web of double-tee slab, which causes structural instability and ultimate failure. However, under the realistic fire exposure, cracking and crushing did not cause failure, which shows that it is important to account for realistic fire exposure.

Future study

The proposed approach can trace the fire response of double-tee slabs from the start of the fire to burnout conditions under any given fire and loading conditions. This approach can be implemented using any FEA computer program, and using such an approach can allow designers and fabricators to develop cost-effective innovative design solutions, which can save time and money compared with costly experimental tests. Whereas the applicability of this approach has been demonstrated for double-tee slabs under vehicle fire exposure in this paper, the same can be extended to other structural members, such as hollow-core and solid slabs. Also, to develop a rational simplified design approach for slabs under vehicle fire exposure, a series of parametric studies is needed to investigate the influence of the cooling rate of fire, vehicle burning duration, location of fire exposure, load level, restraint conditions, length of slab, and so forth. A detailed study on these aspects is in progress at Michigan State University.

Conclusion

Based on the information presented in this paper, the following conclusions can be drawn:

- A fire scenario in a parking structure resulting from a vehicle fire is significantly different from building fires. Fire severity in a parking structure primarily depends on the number of vehicles involved in the fire, the location of the combustion in the vehicle or vehicles, the quantity of combustible fuel in the vehicle or vehicles, the spacing between vehicles, the spread of fuel, and the ventilation conditions.
- Vehicle fire scenarios involving one to three vehicles make up about 96% of documented fires in parking structures, and most vehicle fires attain burnout condition in less than 60 minutes.
- Double-tee slabs can withstand typical vehicle fire scenarios with minimal structural damage because the

high thermal inertia of concrete limits a rapid increase in cross-sectional temperatures. Peak strand temperatures in the case-study slabs remained below 250°C (482°F) and lost only 8.5% of room-temperature strength.

- The use of standard fire exposure to predict the fire resistance of double-tee slabs in parking structures under vehicle fires does not yield a realistic assessment of fire performance.

Acknowledgments

The support of this work by the Daniel P. Jenny Fellowship and Michigan State University is gratefully acknowledged. Any opinions, findings, conclusions, or recommendations expressed in this paper are those of the authors and do not necessarily reflect the views of these institutions.

References

1. ASTM Subcommittee E05.11. 2019. *Standard Test Methods for Fire Tests of Building Construction and Materials*. ASTM E119-19. West Conshohocken, PA: ASTM.
2. Franssen, J. M., and A. Bruls. 1997. "Design and Tests of Prestressed Concrete Beams." In *Proceedings of 5th International Symposium on Fire Safety Science, London*. International Association for Fire Safety Science 1081–1092.
3. Kodur, V., and N. R. Hatinger. 2011. "A Performance-Based Approach for Evaluating Fire Resistance of Prestressed Concrete Double T-Beams." *Journal of Fire Protection Engineering* 21 (3): 185–222. <https://doi.org/10.1177/1042391511417795>.
4. Shakya, A. M., and V. K. R. Kodur. 2015. "Response of Precast Prestressed Concrete Hollowcore Slabs under Fire Conditions." *Journal of Engineering Structures* 87: 126–138. <http://dx.doi.org/10.1016/j.engstruct.2015.01.018>.
5. Kumar, P., and G. Srivastava. 2017. "Numerical Modeling of Structural Frames with Infills Subjected to Thermal Exposure: State-of-the-Art Review." *Journal of Structural Fire Engineering* 8 (3): 218–237. <https://doi.org/10.1108/JSFE-05-2017-0031>.
6. Kodur, V., P. Kumar, and M. M. Rafi. "Fire Hazard in Buildings: Review, Assessment and Strategies for Improving Fire Safety." *PSU Research Review*. Published ahead of print, September 11, 2019. <https://doi.org/10.1108/PRR-12-2018-0033>.
7. Kumar, P., and V. Kodur. 2019. "Numerical Model to Evaluate Fire Resistance of Restrained Prestressed Concrete Beams." Paper presented at PCI Committee Days and Technical Conference, Rosemont, IL, September 2019. https://www.pci.org/PCI_Docs/Papers/2019/5_Final_Paper%20Kumar%20Kodur.pdf.

8. Kodur, V. K. R., and P. Kumar. 2018. "Rational Design Approach for Evaluating Fire Resistance of Hollow Core Slabs Under Vehicle Fire Exposure." Paper presented at PCI Convention and National Bridge Conference, February 2018, Denver, CO. https://www.pci.org/PCI_Docs/Papers/2018/9_Final_Paper.pdf.
9. PCI Industry Handbook Committee. 2017. *PCI Design Handbook: Precast and Prestressed Concrete*. MNL-120. 8th ed. Chicago, IL: PCI.
10. ACI (American Concrete Institute) Committee 216. 2014. *Code Requirements for Determining Fire Resistance of Concrete and Masonry Construction Assemblies*. ACI 216.1-14. Farmington Hills, MI: ACI.
11. Ahrens, M. 2012. "Automobile Fires in the U.S.: 2006–2010 Estimates." In *Second International Conference on Fires in Vehicles: Proceedings, September 27–28, Chicago, IL*. Borås, Sweden: SP Technical Research Institute of Sweden.
12. Li, Y. 2004. "Assessment of Vehicle Fires in New Zealand Parking Buildings." Master's thesis, Department of Civil Engineering, University of Canterbury, New Zealand.
13. Joyeux, D., J. Kruppa, L. G. Cajot, J. B. Schleich, P. Van de Leur, and L. Twilt. 2002. *Demonstration of Real Fire Tests in Car Parks and High Buildings*. Brussels, Belgium: European Commission.
14. Shipp, M., R. Chitty, D. Crowder, R. Cullinan, J. Fraser-Mitchell, and P. Clark. 2010. *Fire Spread in Car Parks*. London, UK: Department for Communities and Local Government.
15. BBC News. 2018. "Liverpool Echo Arena Car Park Fire Photos Released." <http://www.bbc.com/news/uk-england-merseyside-42542556>.
16. Mangs, J., and O. Keski-Rahkonen. 1994. "Characterization of the Fire Behaviour of a Burning Passenger Car. Part I: Car Fire Experiments." *Fire Safety Journal* 23 (1): 17–35. [https://doi.org/10.1016/0379-7112\(94\)90059-0](https://doi.org/10.1016/0379-7112(94)90059-0).
17. Mangs, J., and O. Keski-Rahkonen. 1994. "Characterization of the Fire Behaviour of a Burning Passenger Car. Part II: Parametrization of Measured Rate of Heat Release Curves." *Fire Safety Journal* 23 (1): 37–49. [https://doi.org/10.1016/0379-7112\(94\)90060-4](https://doi.org/10.1016/0379-7112(94)90060-4).
18. Alpert, R. L. 1972. "Calculation of Response Time of Ceiling-Mounted Detectors." *Fire Technology* 8 (3): 181–95.
19. Franssen, J. M., L. Twilt, J. Van Oerle, J. Kruppa, D. Joyeux, and G. Aurtentetxe. 1999. *Development of Design Rules for Steel Structures Subjected to Natural Fires in Closed Car Parks*. EUR 18867. Brussels, Belgium: European Commission.
20. Li, D., G. Zhu, H. Zhu, Z. Yu, Y. Gao, and X. Jiang. 2017. "Flame Spread and Smoke Temperature of Full-Scale Fire Test of Car Fire." *Case Studies in Thermal Engineering* 10: 315–324. <https://doi.org/10.1016/j.csite.2017.08.001>.
21. Zhang, X. G., Y. C. Guo, C. K. Chan, and W. Y. Lin. 2007. "Numerical Simulations on Fire Spread and Smoke Movement in an Underground Car Park." *Building and Environment* 42 (10): 3466–3475. <https://doi.org/10.1016/j.buildenv.2006.11.002>.
22. Tohir, M. Z. M., M. Spearpoint, and C. Fleischmann. 2018. "Prediction of Time to Ignition in Multiple Vehicle Fire Spread Experiments." *Fire and Materials* 42: 69–80. <https://doi.org/10.1002/fam.2458>.
23. Merci, B., and M. Shipp. 2013. "Smoke and Heat Control for Fires in Large Car Parks: Lessons Learnt from Research?" *Fire Safety Journal* 57: 3–10. <https://doi.org/10.1016/j.firesaf.2012.05.001>.
24. Haremza, C., A. Santiago, and L. S. da Silva. 2013. "Design of Steel and Composite Open Car Parks under Fire." *Advanced Steel Construction* 9 (4): 350–368.
25. Bayreuther, J. L., and S. P. Pessiki. 2006. *Analytical Investigation of Fire Loads for Precast Concrete Parking Structures*. ATLSS report 06-19. Bethlehem, PA: Lehigh University. <http://preserve.lehigh.edu/engr-civil-environmental-atlss-reports/84>.
26. CEN (European Committee for Standardization) Technical Committee CEN/TC250. 2004. *Eurocode 2: Design of Concrete Structures—Part 1-2: General Rules—Structural Fire Design*. Brussels, Belgium: CEN.
27. CEN. 2002. *Eurocode 1: Actions on Structures—Part 1-2: General Actions—Actions on Structures Exposed to Fire*. Brussels, Belgium: CEN.
28. Kumar, P., and G. Srivastava. 2018. "Effect of Fire on In-Plane and Out-of-Plane Behavior of Reinforced Concrete Frames with and Without Masonry Infills." *Construction and Building Materials* 167: 82–95. <https://doi.org/10.1016/j.conbuildmat.2018.01.116>.
29. Kumar, P., and V. K. R. Kodur. 2017. "Modeling the Behavior of Load Bearing Concrete Walls under Fire Exposure." *Construction and Building Materials* 154: 993–1003. <https://doi.org/10.1016/j.conbuildmat.2017.08.010>.
30. BSI (British Standards Institution). 1987. *Fire Tests on Building Materials and Structures—Part 20: Method for Determination of the Fire Resistance of Elements of*

Construction (General Principles). BS 476-20. London, UK: BSI.

31. Selvaggio, S. L., and C. C. Carlson. 1963. "Effect of Restraint on Fire Resistance of Prestressed Concrete." In *Symposium on Fire Test Methods* (1962). West Conshohocken, PA: ASTM International. <https://doi.org/10.1520/STP44508S>.
32. Zhao, B., and J. Kruppa. 2004. "Structural Behaviour of an Open Car Park Under Real Fire Scenarios." *Fire and Materials* 28 (2): 269–280. <https://doi.org/10.1002/fam.867>.
33. ASCE (American Society of Civil Engineers). 2017. *Minimum Design Loads and Associated Criteria for Buildings and Other Structures*. ASCE/SEI 7-16. Reston, VA: ASCE.

Notation

a_t	= depth of equivalent rectangular stress block at time t
A_{ps}	= area of prestressing steel
b	= width of slab
b_w	= thickness of web
d	= effective depth of slab
$f_{c\theta,t}$	= compressive strength of concrete evaluated at average cross-sectional concrete temperature θ_a at time t
$f_{c\theta,t}$	= compressive strength of concrete evaluated at average temperature in zone of rectangular stress block θ_c at time t
$f_{c\theta_e}$	= compressive strength of concrete at element temperature θ_e
$f_{ps\theta,t}$	= actual stress in prestressing strands at average strand temperature θ_s corresponding to time t
$f_{pu\theta,t}$	= ultimate stress in prestressing strands at average strand temperature θ_s corresponding to time t
F	= function of principal stress state
L	= length of the slab
M_{nt}	= reduced moment capacity at time t under fire exposure
M_u	= applied moment under fire conditions
S	= continuous failure surface

t	= time under fire exposure
t_{fire}	= total duration of fire exposure
t_s	= incremental time in structural analysis
t_t	= incremental time in thermal analysis
V_{nt}	= reduced shear capacity of a slab at time t under fire exposure
V_u	= applied shear loading under fire conditions
Δt_s	= time increment during structural analysis
Δt_t	= time increment during thermal analysis
θ_a	= average cross-sectional concrete temperature
θ_c	= average temperature in zone of rectangular stress block
θ_e	= element temperature
θ_s	= average strand temperature

About the authors



Puneet Kumar is a PhD student in the department of Civil and Environmental Engineering at Michigan State University in East Lansing, Mich. He is a consulting member on the PCI Fire Committee. He received his master's

degree in structural engineering from the Indian Institute of Technology Gandhinagar. His research interests include fire-performance-based design of precast, prestressed concrete structures.



Venkatesh K. R. Kodur is a university distinguished professor and director of the Center on Structural Fire Engineering and Diagnostics at Michigan State University. His research interests include evaluation of fire resis-

tance of structural systems through large-scale fire experiments, numerical modeling, and characterization of materials under high temperatures. His research contributions have led to the development of a fundamental understanding of the fire behavior of materials and structural systems and have also resulted in numerous design approaches and innovative, cost-effective solutions for enhancing the fire resistance of structural systems. He has published more than 400 peer-reviewed papers in journals and conferences in the areas of structural and fire engineering. He is a fellow of fire institute/academies including American Concrete Institute and Canadian Academy of Engineering.

Abstract

A rational approach for evaluating the fire resistance of double-tee, prestressed concrete slabs in parking structures is proposed in this paper. The approach is implemented through a finite element analysis (FEA) numerical model to evaluate the fire resistance of double-tee slabs under varying fire and loading scenarios that could occur in a parking structure. The FEA model accounts for varying fire characteristics, member geometry, loading and support conditions, temperature-dependent material properties, and realistic failure limit states to evaluate the fire resistance of double-tee slabs. The numerical model is validated by comparing thermal and structural response parameters with measured values from documented fire tests. Furthermore, the model is applied to case studies aimed at quantifying the fire performance of typical double-tee slabs under different vehicle fire exposures in parking structures. Results from these numerical studies clearly indicate that fire-resistance predictions for double-tee slabs under current prescriptive approaches for evaluating fire resistance are overly conservative. Application of the rational approach yields higher fire resistance for double-tee slabs under realistic fire and loading conditions.

Keywords

Double-tee slab, FEA, finite element analysis, fire resistance, parking structure, vehicle fire.

Review policy

This paper was reviewed in accordance with the Precast/Prestressed Concrete Institute's peer-review process.

Reader comments

Please address any reader comments to *PCI Journal* editor-in-chief Tom Klemens at tklemens@pci.org or Precast/Prestressed Concrete Institute, c/o *PCI Journal*, 200 W. Adams St., Suite 2100, Chicago, IL 60606. [P](#)